ELSEVIER

Journal of Crystal Growth 242 (2002) 45–54

JOURNAL OF CRYSTAL GROWTH

www.elsevier.com/locate/jcrysgro

Wetting angles and surface tension of $Ge_{1-x}Si_x$ melts on different substrate materials

A. Cröll[a,b,*], N. Salk[c,b], F.R. Szofran[d], S.D. Cobb[d], M.P. Volz[d]

[a] *Institut für NE-Metallurgie und Reinststoffe, University of Freiberg, Leipziger Strasse 23, D-09599 Freiberg, Germany*
[b] *AMMSA, University of Alabama in Huntsville, SD46, NASA-MSFC, Huntsville, AL 35812, USA*
[c] *Kristallographisches Institut, University of Freiburg, Hebelstr. 25, D-79104 Freiburg, Germany*
[d] *SD46, NASA Marshall Space Flight Center, Huntsville, AL 35812, USA*

Received 1 February 2002; accepted 8 April 2002
Communicated by T. Hibiya

Abstract

The wetting angles and surface tension of $Ge_{1-x}Si_x$ melts ($0.02 < x < 0.13$) have been measured on various substrate materials using the sessile drop technique. Fused quartz, sapphire, SiC, glassy carbon, pBN, AlN, and Si_3N_4 were used as substrates. The highest and most stable wetting angles were found for pBN substrates with $164 \pm 8^\circ$, either under forming gas with an additional carbon getter in the system or under active vacuum. The surface tension measurements resulted in a value of $+2.2 \times 10^{-3}$ N/m at% Si for the concentration dependence $\partial\gamma/\partial C$. For the composition range measured, the temperature dependence $\partial\gamma/\partial T$ showed values similar to those of pure Ge, on average -0.07×10^{-3} N/m K.

PACS: 68.03.Cd; 68.08.Bc; 81.05.Cy

Keywords: A1. Solutocapillary convection; A1. Surface tension; A1. Thermocapillary convection; A1. Wetting angle; A2. Detached Bridgman technique; A2. Floating zone technique; B1. Germanium silicon alloys

1. Introduction

In recent years, the germanium–silicon system has become a material of interest for high-speed electronic devices such as HBTs or HBFETs. Other applications include: thermoelectric converters, X-ray and neutron optics, and solar cells. While several applications use epitaxial films on Si, bulk single crystals are necessary for certain applications. They are also preferable as substrates for epitaxial layers when the composition is neither close to the Si nor to the Ge side of the system.

The Ge–Si system shows complete solid solubility over the entire composition range, but has a large separation between the liquidus and the solidus curves, resulting in strong segregation. This factor, as well as the considerable lattice mismatch between Si and Ge (4%) and the reactivity of

*Corresponding author. Institut für NE-Metallurgie und Reinststoffe, University of Freiberg, Leipziger Strasse 23, D-09599 Freiberg, Germany. Tel.: +49-3731-392017; fax: +49-3731-392268.

E-mail address: arne.croell@inemet.tu-freiberg.de (A. Cröll).

0022-0248/02/$ - see front matter
PII: S0022-0248(02)01347-7

liquid Si, leads to severe difficulties in growing single crystals with low dislocation densities and a homogeneous composition. In addition to Czochralski (CZ) growth, floating-zone (FZ) growth and the so-called "detached Bridgman" growth are currently investigated for the Ge–Si system, with the intent to avoid or reduce the contamination and stress introduced by crucibles.

In detached Bridgman growth, the bulk of the melt is still in contact with the crucible, but a small gap exists between crystal and crucible. The melt adjacent to the growth interface "detaches" from the crucible wall and forms a small free meniscus connecting to the crystal. Detached growth has occasionally been observed for more than 20 years, especially in microgravity, but the mechanisms involved are still the topic of several studies. Overviews can be found in Refs. [1,2]. There is, however, a common understanding that the main factors influencing detachment include pressure differences between the volume below the meniscus and the volume above the melt, a high growth angle, and a high wetting angle between the material and the crucible. One current investigation looks at detached Bridgman growth in the Ge–Si system [3,4], making wetting angles of $Ge_{1-x}Si_x$ melts with a variety of crucible materials quite important for the investigation.

It has been shown by a variety of experiments and numerical simulations that—with the exception of RF-heated industrial-scale Si-FZ growth—mass transport in semiconductor FZs is dominated by surface-tension-driven *thermo*capillary ("Marangoni") convection [5–8]. Recent results on the FZ growth of Ge–Si also suggest that *soluto*-capillary convection, caused by the compositional dependence of the surface tension, plays an equally important role in this system [9]. Knowledge of the surface tension γ as well as its temperature and composition dependencies $\partial\gamma/\partial T$ and $\partial\gamma/\partial C$ are thus essential for designing and understanding FZ experiments and for conducting numerical simulations; they are also important for CZ growth.

Surface tension data exist in the literature for molten Ge [10–20] and Si [21–31], but so far only two values for intermediate compositions have been published [32]. Some values exist for the wetting angles of Ge [14,20,33,34] and Si [14,23,35–43] with different substrates, but none for $Ge_{1-x}Si_x$ melts. The data for the pure elements vary considerably, in particular the temperature dependence of the surface tension; this is due to different levels of contamination, especially by oxygen [23,44,45]. In the following, the results of new sessile drop measurements of $Ge_{1-x}Si_x$ melts will be presented. This method is not free of contamination by the substrate, but allows the parallel determination of surface tension and wetting angle and actually resembles closely the conditions of detached Bridgman crystal growth.

2. Experimental setup

The setup and experimental procedure have been described in detail in a previous article on the wetting angles and surface tension of Ge [20]. The substrates used for the $Ge_{1-x}Si_x$ experiments were plates ($25 \times 25\,mm^2$) of fused quartz, sapphire (Saphikon), pBN (Performance Materials), ceramic AlN (Accuratus), glassy-carbon-coated graphite (Graphite Die Mold), SiC-coated SiC (SuperSiC® from Poco Graphite), ceramic Si_3N_4 (Ceradyne Ceralloy 147), and a CVD Si_3N_4 layer on fused quartz. The choice of substrates was governed by the condition that the material should be available as a cylindrical ampoule or ampoule liner for detached growth experiments. All substrate plates were rinsed in acetone and methanol, the fused quartz and sapphire plates also in a cleaner for lab glassware (Dri-Contrad®) and 13 MΩ water. All parts were then baked out under dynamic vacuum at 1090°C for at least 2 h. The Ge–Si sample consisted of two Ge plates and one or two Si plates sandwiched together (Fig. 1). No pre-synthesized samples were used to avoid contamination by an additional crucible. The plates were cut from single crystals (Eagle-Picher, optical grade, for both Ge and Si), and then etched in a mixture of 18 parts HNO_3 (69%), 8 parts CH_3COOH (100%), and 5 parts HF (49%). Immediately before the sample was put into the vacuum system, the Si was immersed in a 5% HF solution, the Ge in a 20% KOH solution to reduce native oxides, then rinsed in 13 MΩ water. The samples were heated up to the melting point under

Fig. 1. Left: sample before melting, consisting of a Ge–Si–Ge sandwich on a pBN substrate. Ge disk diameter 12 mm. Right: sample after melting in forming gas atmosphere. Si content 5.9 at%.

dynamic vacuum (2×10^{-6} mbar). After melting, the samples stayed at a temperature of 10–20°C above the melting point for several hours to ensure a homogeneous composition, but pictures were already taken during this equilibration time. Dynamic vacuum conditions, 1040 mbar Argon (5N, further purified by Oxisorb® from MG Industries), and 1040 mbar spectral grade forming gas (Ar with 2% H_2) have been employed as atmosphere. No continuous gas flow was used, but the processing chamber was flushed several times before the final filling. This approach was used to simulate the conditions in a sealed growth ampoule. In several runs, an additional carbon plate was placed behind the substrate as an oxygen getter. In each case, measurements were taken at different temperatures, usually in 10–20 K intervals between the melting temperature and the maximum attainable temperature of 1100°C. In some runs, measurements were taken over several days (the usual processing time for Bridgman growth of $Ge_{1-x}Si_x$ crystals) to detect slow reactions with the substrate or the atmosphere that might affect either the surface tension or the wetting angle.

A description of the drop image evaluation using the Young–Laplace equation is given in Ref. [20]. One experimental problem with respect to the evaluation is the knowledge of the exact magnification, since it directly affects the calculation of the surface tension. The magnification can easily be determined for the solid starting material, but upon melting the sample usually moves a little in an arbitrary direction, up to a few tenths of a millimeter. This is often not detectable through a change in focus—the calculated depth of field was ±1 mm for the setup. To overcome this problem, the drop density was used to adjust the magnification. First a theoretical density was calculated for a given temperature T from the densities of the melt constituents: the density value for Ge was calculated using the function $\rho_{Ge}=5.67\,g\,cm^{-3}-5.42\times10^{-4}\,g\,cm^{-3}\,K^{-1}\cdot(T-T_m)$ [19], the value for Si using $\rho_{Si}=2.58\,g\,cm^{-3}-1.59\times10^{-4}\,g\,cm^{-3}\,K^{-1}\cdot(T-T_m)-1.15\times10^{-7}\,g\,cm^{-3}\,K^{-2}\cdot(T-T_m)^2$ [31], with T_m as the melting temperatures (938°C for Ge, 1414°C for Si). The theoretical density for the alloy was then calculated by linearly interpolating between the two component densities, and the magnification was adjusted so that the experimental value matched the theoretical one within $\pm0.005\,g\,cm^{-3}$.

After processing the samples were cooled down and checked for surface contamination as well as for adherence to the substrate. Selected samples were checked for impurities by EDX and glow discharge mass spectrometry (GDMS).

3. Results and discussion

3.1. Wetting angles of $Ge_{1-x}Si_x$ melts with different substrates

A general result was that wetting angles were reduced over time for all substrates except pBN. This is different from the results for pure germanium, where this happened only for some substrates [20]. The high reactivity of (liquid) silicon is most probably responsible for this effect,

leading to a reaction with the substrate and thus changing both the drop composition and the substrate surface texture. The rate of change was generally highest for the oxide-based substrates (fused quartz and sapphire) and depended also on the surrounding atmosphere. No significant temperature dependence of the wetting angle could be found for any of the substrates within the temperature range used (up to 130 K, depending on composition).

3.1.1. Fused quartz substrates

The wetting angle for pure Si is reported to be 85–87° [38,41,43], the one for pure Ge is in the range 120–140°, depending on the surrounding atmosphere [20]. The values for $Ge_{1-x}Si_x$, with Si contents of 3.3%, 3.4%, 6.6%, and 10.7%, fall between these extremes, as shown in Table 1. At the beginning of the experiment, the initial values were closer to the ones for pure Ge and then approached asymptotically a limiting value (Fig. 2). This exponential decay was faster with increasing Si content. Similar to the Ge results [20], the wetting angles measured under vacuum are 15–20° lower than those measured under argon/forming gas. The samples processed under vacuum and the one processed with additional carbon getter in the system showed no macroscopically detectable surface contamination, whereas the sample processed under forming gas alone showed visible formation of solid particles after 2 days of processing. The solidified samples adhered to the substrate in all cases, resulting in the destruction of the substrate and sometimes the sample upon cooling down. This attests to the strong reaction of the melt with the substrate, which is corroborated by the high oxygen content found in parts of the samples, around 16 ppm for a vacuum-processed sample (Table 2).

3.1.2. Sapphire substrates

The sapphire substrate measurements resulted in angles of 114–124°, similar to fused quartz (Table 1). This is just slightly below the pure Ge

Table 1
Wetting angles of $Ge_{1-x}Si_x$ on various substrates, for different compositions and processing atmospheres

Substrate	Si content (%)	Processing atmosphere	Wetting angle (°)
Fused quartz	3.3	Forming Gas	128 → 122
	3.4	Vacuum	130 → 105
	6.6	Forming gas + carbon getter	128 → 117
	10.7	Vacuum	→ 100
Sapphire	4.2	Vacuum/argon	→ 124
	4.6	Vacuum/forming gas	127 → 114
SiC	6.5	Vacuum/argon	165 → 70
Glassy carbon	3.1	Forming gas	160 → 120
	4.6	Vacuum	150 → 103
AlN	6.3	Vacuum/argon	168 → 124
Si_3N_4 layer on SiO_2	5.7	Vacuum	160 → 97
Ceramic Si_3N_4	6.2	Vacuum/argon	153 → 96
PBN	2	Vacuum	163 ± 1*
	2.2	Vacuum/argon	159 ± 1*
	7.1	Vacuum/argon	168 ± 2*
	2.3	Forming gas + carbon getter	167 ± 4*
	4.3	Forming gas	166 ± 3*
	5.9	Forming gas + carbon getter	173 → 162*
	6.5	Forming gas + carbon getter	148 ± 1*
	11.4	Argon + carbon getter	171 ± 2*
	13.6	Forming gas + carbon getter	174 ± 2*

→ Denotes a change of the wetting angle over time following an exponential decay law (Figs. 2 and 4). The error for the wetting angles (for the cases without a systematic change of the angle) is the standard deviation. The average value of the marked * angles on pBN is 164° with a standard deviation of ±8° between those values.

values of 119–134° [20], whereas literature values for Si melts are 80–86° [14,38]. The measurements under argon or forming gas resulted in the formation of particles on the surface; in contrast to fused quartz substrates, there was no increase of the angle when going from vacuum to a gas atmosphere. The samples also adhered strongly to the substrate after processing.

3.1.3. SiC substrates

The wetting angle for SiC started at 165°, which is essentially the value for Ge [20], but then decreased rapidly within 1 h to values below 90°. It stabilized around 70° (Table 1) and stayed there for up to 3 days. No change could be found for vacuum vs. argon atmosphere. This low angle is not too surprising, given the fact that the angle for pure Si on SiC is reported to be between 8° and 50°

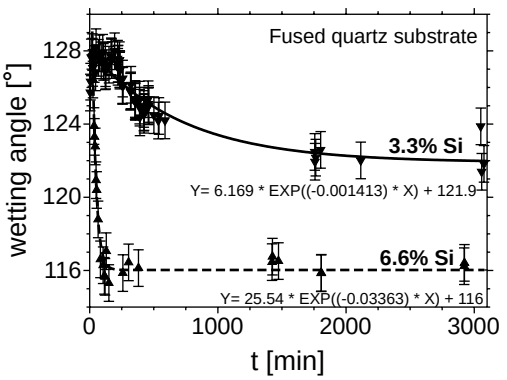

Fig. 2. Wetting angles for a $Ge_{0.967}Si_{0.033}$ drop and a $Ge_{0.934}Si_{0.066}$ drop vs. time, fused quartz substrates, forming gas atmosphere. The higher Si content leads to a faster decay of the initial angle and to a lower stable angle as well. Error bars show the standard deviation.

[14,38]. The samples adhered strongly to the substrate after processing and could not be removed without destroying them. SiC was the only substrate that showed wetting, i.e. a wetting angle below 90°.

3.1.4. Glassy-carbon-coated graphite substrates

The wetting angle of pure Ge on carbon is around 160–170° [20], whereas the value for Si has been reported to be between 10° and 50° [39,40,43]. It can be safely assumed that this range is actually the wetting angle of Si with SiC due to the reaction of the melt with the carbon. For the Ge–Si melts, the behavior was similar to the one with the SiC substrate. Initial wetting angles were quite high at 150–160°, in the vicinity of the pure Ge values, and then decreased to values of 110° and 120° within a day. There was no apparent influence of the processing atmosphere. The samples also adhered permanently to the substrates after processing, but did not show visible contamination of the sample surface. One would assume that also for $Ge_{1-x}Si_x$ the measured values represent to a large extent the wetting angle with SiC, i.e. the substrate surface in contact with the melt is SiC, and outside that area it is carbon. The drop could then advance by diffusion of Si, forming new SiC along the perimeter of the contact area. As long as the drop is advancing, the contact line would, therefore not be a three-phase (solid–liquid–gas) contact line, but closer to a four-phase (solid–solid–liquid–gas) contact line.

3.1.5. AlN substrates

The wetting angle for AlN started out at a very high value, 168°, close to that of Ge, but then

Table 2
GDMS measurements of $Ge_{1-x}Si_x$ selected sessile drops on different substrate materials after processing. Elements not listed showed no significant increase in concentration

Substrate	Si content (%)	Processing atmosphere	Processing time (h)	B (ppb)	C (ppb)	N (ppb)	O (ppb)
Fused quartz	3.4	Vacuum	52	<4	300	130	16000
Glassy carbon	4.6	Vacuum/argon	47	17	740	120	1700
pBN	2	Vacuum	7	90	520	200	3300
pBN	2.2	Vacuum	126	3900	230	120	2100

decreased within a day to 124° (Table 1) and stayed there for another 3 days of processing. For comparison, angles of 45–60° are reported for pure Si [14,37]. It has to be kept in mind that ceramic AlN contains several % of additives, i.e. Y_2O_3, Al_2O_3, or MgO, so this decrease may be due to the oxide content. No surface contamination of the drop was visible and no change of the angle could be found for vacuum vs. argon atmosphere. The samples did not adhere to the substrate after processing and could be removed easily.

3.1.6. Si_3N_4 substrates

Si_3N_4 was an interesting candidate as ampoule material or coating since it would only introduce nitrogen as a contaminant (for pure Si_3N_4), and it has been reported to be durable in molten Si [42]. The wetting angle for Ge is around 145° under vacuum [20], but for Si values of only 23–85° have been reported [35,37,38,42]. For $Ge_{1-x}Si_x$, the measurements showed initial values around 150°, but those fell quickly, attaining a stable value of 96° (Table 1) after 3 h of processing time (Fig. 4). The results were practically identical for the ceramic material (containing several % of additives like Y_2O_3, Al_2O_3, and MgO) and the CVD layer, so an influence of the ceramic binder on the wetting angle is unlikely. No visible surface contamination of the drops has been found and there was no apparent influence of the processing atmosphere on the angle. The sample adhered permanently to the ceramic substrate after processing.

3.1.7. pBN substrates

Pyrolytic boron nitride was the most likely candidate to exhibit high wetting angles, since the value for Ge is around 170° [20] and the value for Si is reported to be 130–145° [23,38]. pBN did indeed exhibit the highest wetting angles of all substrates (Table 1). The angles obtained under vacuum and under forming gas were the highest with values around 150–170°, similar to pure Ge melts. For most samples processed under forming gas and with additional carbon getter, the reduction of the angle with time is practically negligible (Fig. 3). They still showed significant data scattering from run to run; the average value for the

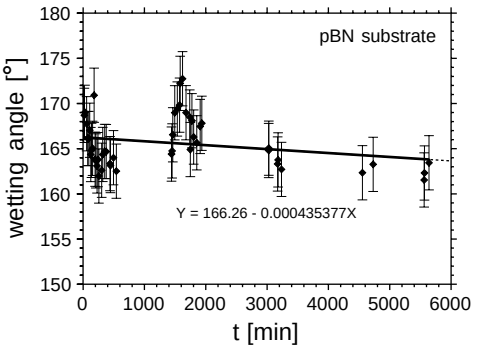

Fig. 3. Wetting angle for a $Ge_{0.966}Si_{0.034}$ drop vs. time, pBN substrate, forming gas atmosphere. The change of the angle is less than 1° per day. Error bars show the standard deviation.

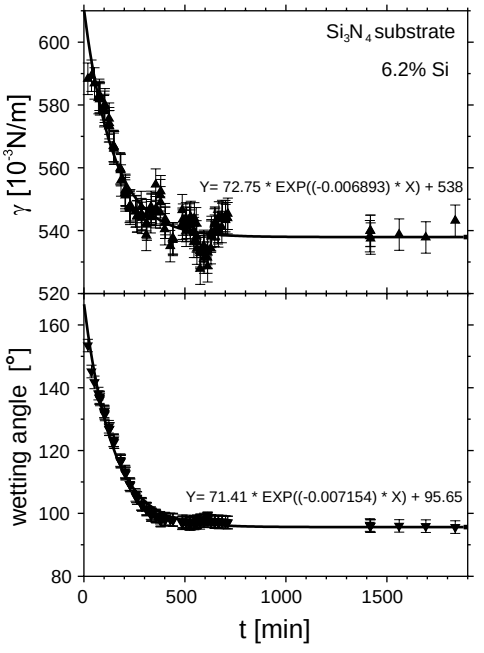

Fig. 4. Wetting angle (bottom) and surface tension (top) for a $Ge_{0.938}Si_{0.062}$ drop vs. time, Si_3N_4 substrate. Atmosphere: dynamic vacuum up to $t = 442$ min, then 5 N Ar. The peaks in the surface tension around $t = 300$ and 600 min are due to intentional temperature changes. Error bars show the standard deviation.

samples processed under vacuum or forming gas was 164°, with a standard deviation of $\pm 8°$ between the runs. These samples did not show any visible contamination. No significant dependence

of the angle on the Si content was found. After solidification, the samples could easily be removed from the substrate, which showed no visible sign of dissolution. However, the GDMS analysis showed a dependence of the incorporation of boron into the sample on the processing time, up to 3.9 ppm (equivalent to a doping level of $2 \times 10^{17}\,\mathrm{cm}^{-3}$) after 5 days of processing; no significant amounts of nitrogen where detected (Table 2). For samples processed only under argon, smaller wetting angle values were found after some processing time and a transparent layer of material of a few micron thickness was found on the substrate. The layer appears to be mainly SiO_2, not B_2O_3, since it could not be readily dissolved in a KOH solution. In this case, the measured lower wetting angle is related to the one for SiO_2, not pBN.

3.2. Surface tension of $Ge_{1-x}Si_x$ melts

The surface tension results are summarized in Table 3. See Ref. [20] for details on the related sessile drop measurements of pure Ge melts. In contrast to the wetting angles, an asymptotic change of the surface tension over time was found only for the ceramic Si_3N_4 substrate with a reduction of 10% within 8 h (Fig. 4). This is similar to the results for pure Ge [20]. Excepting Si_3N_4, the measurements on glassy carbon resulted generally in smaller absolute surface tension values than for the other substrates (Table 3), in accordance with the results for pure Ge [20]. This effect cannot be attributed to the substrate acting as an oxygen getter, since measurements on other substrates with a carbon plate behind the sample acting as a getter did not show the reduced surface tension values.

The processing atmosphere, especially the use of argon without any additional oxygen getter, had an influence on the surface tension values; those effects were somewhat irreproducible and should be related to surface contamination. Going from dynamic vacuum to an argon atmosphere resulted in an increase of the apparent surface tension with oxygen-based substrates. Contamination effects also showed up in the temperature dependence of the surface tension, resulting in different coefficients for runs where the temperature was increased vs. runs where the temperature was decreased. The values for $\partial\gamma/\partial T$ shown in Table 3 and in the examples in Fig. 5 are those with *reproducible* values for the temperature dependence of the surface tension, i.e. from runs under vacuum or in a reducing environment.

It should be noted that the absolute values of the surface tension γ listed in Table 3 are not the ones at the melting point, because the melting point is obviously composition dependent, but have been normalized for a temperature of 1090°C. The choice of 1090°C is arbitrary and only related to the temperature limits of our furnace.

Table 3
Surface tension and its temperature dependence for $Ge_{1-x}Si_x$ melts on fused quartz, glassy carbon, and pBN substrates

Substrate	Si content (%)	Processing atmosphere	γ and $\partial\gamma/\partial T$ (10^{-3} N/m) (T =1090°C)	σ_n (10^{-3} N/m)
Fused quartz	6.6	Forming gas + carbon getter	571, −0.144	2
Glassy carbon	3.1	Forming gas	555, −0.067	1.5
	4.6	Vacuum	558, −0.111	1.5
pBN	2.3	Forming gas + carbon getter	586, −0.062	2
	5.9	Forming gas + carbon getter	**572, −0.081**	1.5
	6.5	Forming gas + carbon getter	**572, −0.061**	1.5
	7.1	Vacuum	**573, −0.045**	0.5
	11.4	Argon + carbon getter	**578, −0.104**	0.5
	13.6	Forming gas + carbon getter	**591, −0.069**	1

The absolute values were normalized for a temperature of 1090°C. σ_n is the standard deviation of the linear fit for each measurement series. Boldface numbers have been used to determine $\partial\gamma/\partial C$ (Fig. 6); the standard deviation of those values from a linear fit is 3.5×10^{-3} N/m.

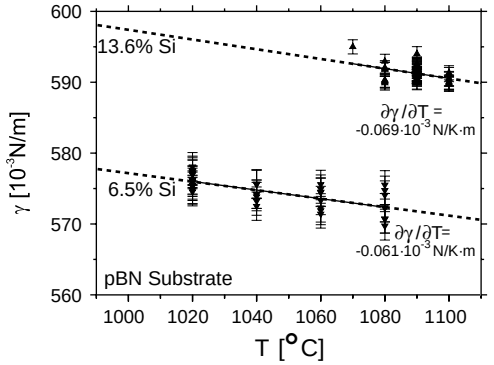

Fig. 5. Temperature dependencies of surface tension for a $Ge_{0.935}Si_{0.065}$ drop (lower graph) and a $Ge_{0.864}Si_{0.136}$ drop (upper graph) vs. temperature; pBN substrates forming gas atmosphere. Error bars show the standard deviation.

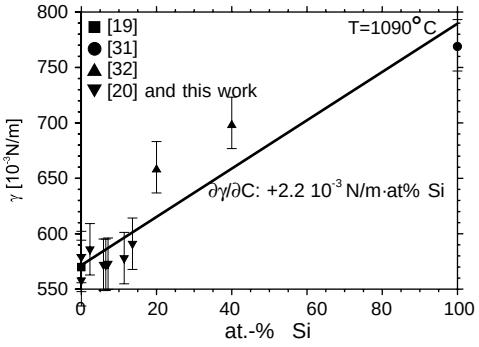

Fig. 7. Concentration dependence of the surface tension for $Ge_{1-x}Si_x$ ($0<x<1$), using literature values for Ge [19,20] and Si [31] and two intermediate Si concentrations [32], as well as the measured values from Table 3. The values are again normalized for a temperature of 1090°C. Error bars show the standard deviation.

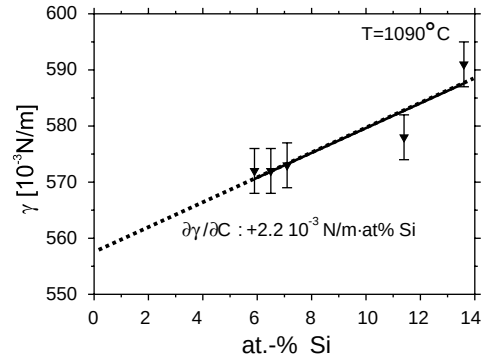

Fig. 6. Concentration dependence of the surface tension for $Ge_{1-x}Si_x$ ($0.05<x<0.14$). The values were normalized for a temperature of 1090°C using γ and $\partial\gamma/\partial T$ from Table 3. Error bars show the standard deviation.

The concentration dependence of the surface tension, shown in Fig. 6, was derived from those results. It was established in the following way: Only measurements on pBN were used. γ and $\partial\gamma/\partial T$ were measured for each composition ($x > 0.05$), as listed in Table 3. γ was calculated from these results for 1090°C, and $\partial\gamma/\partial C$ was determined from this set of calculated γ values. Assuming a linear relationship, $\partial\gamma/\partial C$ was determined to be $+2.2\times10^{-3}$ N/m at% Si. This value compares well with a linear regression using the end values of pure Ge [19,20] and Si [31], as well as the available $Ge_{1-x}Si_x$ values [32], resulting also in 2.2×10^{-3} N/m at% Si (Fig. 7). The standard deviation of the individual surface tension measurements is quite small (Table 3). However, this accounts only for statistical errors, not for systematic ones. According to Eustathopoulos [14], an error of 5% for the absolute surface tension values of metallic melts and of 50% for the temperature dependence is common. Since $\partial\gamma/\partial C$ was derived from $\partial\gamma/\partial T$ values, the error for the concentration dependence is probably in the same order of magnitude, i.e. roughly $\pm1\times10^{-3}$ N/m at% Si.

4. Summary and conclusions

Wetting angles of Ge-rich Ge–Si melts on different substrate materials were determined using the sessile drop technique. Compared to pure germanium [20], reactions with the substrate were much more pronounced. This can be attributed to the high reactivity of silicon. Changes of the wetting angle with time were found for fused quartz, sapphire, glassy carbon, SiC, AlN, and Si_3N_4 substrates. Only pBN substrates showed a negligible reduction of the wetting angle for process times of the order of days. Wetting angles for $Ge_{1-x}Si_x$ melts were generally smaller than for

pure Ge, and most showed significant discrepancies with a linear interpolation between the literature values of Ge and Si. This can again be attributed to the reactivity of liquid silicon, despite the fact that the processing temperatures were more than 300 K below the melting point of Si. The only exceptions to this behavior were pBN substrates. pBN showed the highest values of the wetting angle, around 164°, although only for samples processed under vacuum or in a reducing atmosphere, and with considerable scatter of data. For detached Bridgman growth of $Ge_{1-x}Si_x$ crystals, pBN appears to be the best ampoule liner material. However, even in this case some reaction of the melt with the substrate was found, leading to boron contamination in the ppm range after several days of processing.

In addition to the wetting angle, the surface tension and its concentration and temperature dependence were determined. A pronounced effect of contamination on the surface tension was found for Si_3N_4 substrates. The most reliable surface tension values were measured on pBN substrates either under dynamic vacuum or under forming gas and with carbon as oxygen getter. The temperature dependence $\partial\gamma/\partial T$ (average value -0.07×10^{-3} N/m K) did not differ significantly from that of pure germanium (-0.08×10^{-3} N/m K [19,20]). The concentration dependence $\partial\gamma/\partial C$ was determined to be $+2.2 \times 10^{-3}$ N/m at% Si and agrees well with a linear interpolation between the values of pure Ge and Si. This value, coupled with the strong segregation in the system Ge–Si, can lead to solutocapillary convection during crystal growth with a free melt surface, i.e. in the case of floating-zone or Czochralski growth. Since the segregation coefficient of Si in Ge is much larger than one, this will lead to a *soluto*capillary surface flow away from the interface (i.e. towards the higher Si concentration in the bulk of the melt) which is opposite to the *thermo*capillary flow pointing towards the interface. Recent results [9] show that in the case of FZ-grown $Ge_{1-x}Si_x$ crystals solutocapillary convection can indeed be the dominating flow in the area close to the interface and the melt surface and will lead to a change in the interface shape of the crystal.

Acknowledgements

The authors are indebted to C. Bahr, J. Quick, and D. Lovell for building and maintaining the sessile drop system, and to W. Fernandez and S. Fowler for evaluation of the drop pictures. The GDMS measurements were performed by A. Mykytiuk at the National Research Council Canada. Thanks are also due to P. Dold and M. Schweizer for many invaluable discussions. This work was funded by the NASA Physical Sciences Division as part of the ISS flight project "Reduction of Defects in Germanium–Silicon (RDGS)".

References

[1] T. Duffar, P. Boiton, P. Dusserre, J. Abadie, J. Crystal Growth 179 (1997) 397.
[2] L.L. Regel, W.R. Wilcox, Microgravity Sci. Technol. 11 (1999) 152.
[3] F.R. Szofran, M.P. Volz, M. Schweizer, N. Kaiser, S.D. Cobb, A. Cröll, P. Dold, Proceedings of the Conference on ISS Utilization 2001, AIAA 2001-5002, Kennedy Space Center, Florida, October 15–18, 2001.
[4] M. Schweizer, S.D. Cobb, M.P. Volz, J. Szoke, F.R. Szofran, J. Crystal Growth 235 (2002) 161.
[5] A. Eyer, H. Leiste, R. Nitsche, Proceedings of the Fifth European Symposium on Materials Sciences under Microgravity, Schloß Elmau 1984, p. 17.
[6] A. Cröll, W. Müller-Sebert, K.W. Benz, R. Nitsche, Microgravity Sci. Technol. III/4 (1991) 204.
[7] G. Müller, R. Rupp, Crystal Properties and Preparation 35 (1991) 138.
[8] Th. Kaiser, K.W. Benz, J. Crystal Growth 183 (1998) 564.
[9] T.A. Campbell, M. Schweizer, P. Dold, A. Cröll, K.W. Benz, J. Crystal Growth 226 (2001) 231.
[10] V.I. Davydov, Germanium, Gordon and Breach Science Publishers, New York, 1966.
[11] V.M. Glazov, S.N. Chizhevskaya, N.N. Glagoleva, Liquid Semiconductors, Plenum Press, New York, 1969.
[12] C. Allen, The surface tension of liquid metals, in: S.Z. Beer (Ed.), Liquid Metals, Chemistry and Physics, Marcel Dekker, New York, 1972.
[13] S. Nakamura, T. Hibiya, Int. J. Thermophys. 13 (1992) 1061.
[14] N. Eustathopoulos, M.G. Nicholas, B. Drevet, Wettability at high temperatures, Pergamon, Amsterdam, 1999.
[15] P.H. Keck, W.V. Horn, Phys. Rev. 91 (1953) 512.
[16] L.B. Lazarev, Teoreticheskaya I Eksperimental'naya Khimiya 3 (1967) 504.
[17] M. Brunet, J.C. Joud, N. Eustathopoulos, P. Desre, J. Less Common Mater. 51 (1977) 69.

[18] H. Nakanishi, K. Nakazato, S. Asaba, K. Abe, S. Maeda, K. Terashima, J. Crystal Growth 187 (1998) 391.
[19] W.K. Rhim, T. Ishikawa, Int. J. Thermophys. 21 (2000) 429.
[20] N. Kaiser, A. Cröll, F.R. Szofran, S.D. Cobb, K.W. Benz, J. Crystal Growth 231 (2001) 448.
[21] S.N. Zadumkin, Sov. Phys. Solid State 1 (1959) 516.
[22] S.V. Lukin, V.I. Zhuchkov, N.A. Vatolin, Y.U.S. Kozlov, J. Less Common Metals 67 (1979) 407.
[23] S.C. Hardy, J. Crystal Growth 69 (1984) 456.
[24] M. Przyborowsky, T. Hibiya, M. Eguchi, I. Egry, J. Crystal Growth 151 (1995) 60.
[25] X. Huang, S. Togawa, S.I. Chung, K. Terashima, S. Kimura, J. Crystal Growth 156 (1995) 52.
[26] Z. Niu, K. Mukai, Y. Shiraishi, T. Hibiya, K. Kakimoto, Proceedings of the Fourth Asian Thermophysical Properties Conference, Tokyo 1995, p. 73.
[27] W.K. Rhim, S.K. Chung, A.J. Rulison, R.E. Spjut, Proceedings of the Fourth Asian Thermophysical Properties Conference, Tokyo 1995, p. 353.
[28] H. Sasaki, Y. Anzai, X. Huang, K. Terashima, S. Kimura, Jpn. J. Appl. Phys. 34 (1995) 414.
[29] H. Nakanishi, K. Nakazato, K. Terashima, Jpn. J. Appl. Phys. 39 (2000) 6487.
[30] K. Mukai, Z. Yuan, K. Nogi, T. Hibiya, ISIJ Int. 40 (2000) S148.
[31] W.K. Rhim, K. Ohsaka, J. Crystal Growth 208 (2000) 313.
[32] Y. Takamura, T. Aoyama, K. Kuribayashi, Proceedings of the Spacebound 97, Montreal, 1997, p. 229.
[33] Y.V. Naidich, G.M. Nevodnik, Inorganic Mater. 5 (1969) 1759.
[34] K. Nogi, K. Ogino, Trans. Jpn. Inst. Metals 29 (1988) 724.
[35] M.T. Duffy, S. Berkman, G.W. Cullen, R.V. d'Aiello, H.I. Moss, J. Crystal Growth 50 (1980) 347.
[36] J.G. Li, H.H. Hausner, J. Eur. Ceram. Soc. 9 (1992) 101.
[37] M.W. Barsoum, P.D. Ownby, in: Surfaces and Interfaces in Ceramic and Ceramic–Metal Systems, Plenum, New York 1981, p. 457.
[38] K. Mukai, Z. Yuan, Mater. Trans. JIM 41 (2000) 338.
[39] Y.V. Naidich, in: Progress in Surface and Membrane Science, Vol. 14, Academic Press, New York, 1981, p. 353.
[40] T.J. Whalen, A.T. Anderson, J. Am. Ceram. Soc. 58 (1975) 396.
[41] R. Sangiorgi, M.L. Muolo, D. Chatain, N. Eustathopoulos, J. Am. Ceram. Soc. 71 (1988) 742.
[42] T.F. Ciszek, The capillary action shaping technique and its applications, in: J. Grabmaier (Ed.), Crystals, Growth, Properties and Applications, Vol. 5, Springer, Berlin, 1981.
[43] F.V. Wald, Crystal growth of silicon ribbons for terrestrial solar cells by the EFG method, in: J. Grabmaier (Ed.), Crystals, Growth, Properties and Applications, Vol. 5, Springer, Berlin, 1981.
[44] T. Azami, S. Nakamura, T. Hibiya, J. Crystal Growth 223 (2001) 116.
[45] T. Azami, T. Hibiya, J. Crystal Growth 233 (2001) 417.